Functional poly(phenylacetylene)s carrying azobenzene pendants: Polymer synthesis, photoisomerization behaviors, and liquid-crystalline property

Xiao A.-Zhang[a], Hui Zhao[a], Yuan Gao[a], Jiaqi Tong[a], Liang Shan[a], Yufei Chen[a], Shuang Zhang[a], Anjun Qin[a], Jing Zhi Sun[a,*], Ben Zhong Tang[a,b,**]

[a] Department of Polymer Science and Engineering, Institute of Biological and Medical Macromolecules, MOE of Key Laboratory of Macromolecular Synthesis and Functionalization, Zhejiang University, Hangzhou 310027, China
[b] Department of Chemistry, The Hong Kong University of Science & Technology, Clear Water Bay, Kowloon, Hong Kong, China

ABSTRACT

Functional poly(phenylacetylene)s (PPAs) bearing different azobenzene pendants were synthesized in desirable yields and molecular weight by using organorhodium complexes [Rh(diene)Cl]$_2$ as catalysts. The structure of the derived azobenzene-functionalized PPAs was characterized by NMR, IR, and UV spectroscopic techniques. Their photoinduced isomerization behavior was monitored with UV–visible spectroscopy. The thermal stability was evaluated by TGA technique. Polarized optical microscope (POM) observations indicated that the PPAs constructed by linking azobenzene moieties via a longer flexible alkyl spacer to PPA backbone showed typical liquid-crystalline property and the mesophase was assigned to SmA phase. Their phase transition behaviors were further investigated by differential scanning calorimetric (DSC) measurements. The molecular packing modes were analyzed by using X-ray diffraction (XRD) measurement and theoretical simulation. These results revealed some details about the interactions between the polymer backbone, flexible alkyl spacer, and azobenzene functional moiety, which are constructive to design and synthesize novel functional conjugated polymers.

© 2011 Elsevier Ltd. All rights reserved.

1. Introduction

Polyacetylene is the archetypal conjugated polymer [1–3], and its substituted derivatives have demonstrated a spectrum of advanced functions, such as liquid-crystalline and light-emitting properties, photoconductivity, optical nonlinearity, chain helicity, self-assembling ability, and biocompatibility [4–12]. The liquid-crystalline polyacetylenes are one of research topics in our group. We have designed and synthesized a series of liquid-crystalline polyacetylenes, which contain biphenyl, phenylcyclohexyl, phenyl benzoate, cholesteryl, ergosteryl or stigmasteryl as mesogenic cores, and have gained valuable information on the structure–property relationships involved in these polymers [4–6,13–18]. For example, before the systematic investigation on polyacetylene-based polymeric liquid-crystalline, side-chain liquid-crystalline polymers with stiff backbones have received little attention,

because the rigidity of the conjugated polymer backbone was once considered as a diverse factor to the orderly alignment of mesogens and could result in processing difficulties associated with their high thermal transition temperature. In our previous work, however, it was found that the rigid polyacetylene backbones played an active and constructive role in the alignment and packing processes of the mesogenic pendants and the amelioration of thermal stability.

Azobenzene is a well-known mesogenic functionality and azobenzene-containing polymers have been intensively explored over the past two decades due to their versatile properties, including liquid crystallinity [19–45], optical nonlinearity [46–49], surface relief grating (SRG) formation [36–45,50–62], energy transfer [63–68], and self-assembly [69–74]. Upon exposure to UV and visible light, the azobenzene undergoes photoinduced isomerization between the *trans* and *cis* isomers [75–83], which bestows the azobenzene-containing polymers with interesting photoresponsive properties. Of them, homopolymers and copolymers of azobenzene-containing acrylates have gained the most extensive studies due to their facile preparation through free or controlled radical polymerization.

The introduction of azobenzene moieties into the side chain of polyacetylene, however, is an untouched research area. In this work, we report our studies on the poly(phenylacetylene)s (PPAs)

---

carrying azobenzene pendants. By linking the azobenzene and trifluoromethyl-capped azobenzene moieties to the PPA skeleton with proper flexible alkyl spacers, four azobenzene-containing PPAs have been designed and synthesized (Chart 1, P1 and P2). Their chemical structures have been fully characterized. The thermal stability, the photoinduced isomerization behaviors of the azobenzene functionalities in PPAs side chains, and the mesomorphic properties of the monomers and derived polymers are demonstrated.

2. Experimental

2.1. Materials

Tetrahydrofuran (THF; Labscan) was distilled under normal pressure from sodium benzophenone ketyl under nitrogen immediately prior to use. Triethylamine (TEA) was distilled and dried over potassium hydroxide. Other solvents were purified by standard procedures. Aniline (11), 4-(trifluoromethyl)aniline (12), phenol, 1,6-dibromohexane, 1,12-dibromododecane, 4-iodophenol, piperidine, copper (I) iodide, triphenylphosphine, dichlorobis(-triphenylphosphine)palladium(II), and trimethyl-ethynylsilane were purchased from Aldrich and used as received without further purifications. Sodium nitrite, hydrochloric acid, sodium bicarbonate, potassium carbonate, potassium hydroxide, and potassium iodide were purchased from SCRC and used as received. Organorhodium complexes [Rh(nbd)Cl]$_2$ (nbd = 2,5-norbornadiene) and [Rh(cod)Cl]$_2$ (cod = 1,8-cyclooctadiene) were prepared in our laboratories by literature methods [84].

2.2. Instrumentation

The infrared (IR) spectra were measured on a Perkin−Elmer 16 PC FT-IR spectrophotometer. The ^{1}H and ^{13}C NMR spectra were taken in CDCl$_3$ on a Bruker ARX 400 NMR spectrometer. The chemical shifts were reported in ppm on the δ scale, and tetramethylsilane (TMS; $\delta = 0$ ppm) was used as internal reference for the NMR analysis. The UV−vis absorption spectra were recorded on a Milton Roy Spectronic 3000 Array spectrophotometer. Elemental analysis was conducted on a ThermoFinnigan Flash EA1112 apparatus. Mass spectra were measured on a GCT Premier CAB 048 mass spectrometer. Molecular weights (M_w and M_n) and polydispersity indices (PDI or M_w/M_n) of the polymers were tested in THF with a Waters Associate gel permeation chromatography (GPC) system. The molecular weight was calibrated by a set of monodisperse polystyrene standards covering molecular weight range of $10^3–10^7$.

Under a nitrogen atmosphere, the TGA analysis was performed on a Perkin−Elmer Pyris thermogravimetric analyzer TGA 6 at a heating rate of 20 °C/min. The texture of liquid crystal was observed with an Olympus BX 60 polarized optical microscope (POM) equipped with a Linkam TMS 92 hot stage. The images were taken with a DP70 camera (Olympus). Differential scanning calorimetric (DSC) measurements were undertaken using a Setaram DSC 92 at a heating or cooling rate of 10 °C/min ranging from 50 to 250 °C. X-ray diffraction (XRD) measurements were achieved at room temperature on a Philips PW 1830 powder diffractometer using the monochromatized X-ray beam from the nickel-filtered Cu:Kα radiation with a wavelength of 1.5406 Å (scanning rate 0.05 deg/s, scan range 2°−30°). The polymer samples for the XRD measurements were prepared by freezing the molecular arrangements in the liquid-crystalline state with liquid nitrogen. The polymer films were prepared by spin-coating their 1,2-dichloroethane solutions (3.6 mg/mL) onto quartz substrates at a rotation rate of 1500 r/min.

2.3. Monomer synthesis

Monomers 1(m) and 2(m) (m = 6, 12) were prepared according to the synthetic routes shown in Scheme 1. The detailed experimental procedures for the syntheses of compounds 9, 10, 8(m)−3(m) and monomers 1(m), 2(m) are given below.

2.3.1. Synthesis of (E)-4-(phenyldiazenyl)phenol (9)

In a 250 mL round-bottom flask dissolve 11 (0.93 g, 10 mmol) in concentrated hydrochloric acid (37%, 2.5 mL, 30 mmol) and deionized water (20 mL), apply heat if necessary. The temperature was maintained at 0−5 °C in an ice bath, an aqueous solution of sodium nitrite (0.72 g, 10.5 mmol) was added dropwise through a dropping funnel to the cooled solution. After stirring at 0−5 °C for 15 min, an ethanol solution of phenol (0.94 g, 10 mmol) was added slowly, and then the mixture was stirred for 1 h in ice bath. Add sodium bicarbonate to adjust pH to 7, then the mixture was further stirred for 0.5 h. The resultant precipitate was filtered and the crude product was purified by column chromatography using a mixture of petroleum ether and ethyl acetate (10:1 by volume) as eluent. A yellow solid of 9 was obtained in 89.7% yield. ^{1}H NMR (400 MHz, CDCl$_3$, δ, TMS, ppm): 7.86−7.91 (4H, m, ArH ortho to −N=N−), 7.53 (3H, d, ArH meta and para to −N=N−) and 6.98 (2H, d, ArH ortho to phenolic OH).

2.3.2. (E)-4-((4-(trifluoromethyl)phenyl)diazenyl)phenol (10)

This intermediate was prepared from 12 by a procedure similar to that used for preparation of 9. A yellow solid was obtained in 86.5% yield. ^{1}H NMR (400 MHz, CDCl$_3$, δ, TMS, ppm): 7.90−7.97 (4H, m, ArH ortho to −N=N−), 7.77 (2H, d, ArH ortho to CF$_3$) and 6.99 (2H, d, ArH ortho to phenolic OH).

2.3.3. (E)-1-(4-(6-bromohexyloxy)phenyl)-2-phenyldiazene (7(6))

In a 250 mL round-bottom flask equipped with a reflux condenser were placed 1,6-dibromohexane (3.05 g, 12.5 mmol), potassium carbonate (0.76 g, 5.5 mmol) and acetone (20 mL), and then 10 mL acetone solution of 9 (0.99 g, 5 mmol) was added dropwise through a dropping funnel to the refluxing mixture. The resultant mixture was refluxed for 24 h. The solid was removed by filtration and the filtrate was concentrated under reduced pressure. The crude product was purified by column chromatography using a mixture of petroleum ether and ethyl acetate (50:1 by volume) as eluent. A light yellow solid of 7(6) was obtained in 75.5% yield. ^{1}H NMR (400 MHz, CDCl$_3$, δ, TMS, ppm): 7.94 (4H, m, ArH ortho to −N=N−), 7.49 (2H, t, ArH meta to −N=N−), 7.43 (1H, t, ArH para to −N=N−), 7.01 (2H, d, ArH ortho to phenolic group), 4.08 (2H, t, OCH$_2$), 3.43 (2H, t, CH$_2$Br), 1.85−1.95 (4H, d, [CH$_2$]$_2$) and 1.27−1.64 (4H, t, [CH$_2$]$_2$).

2.3.4. (E)-1-(4-(6-bromohexyloxy)phenyl)-2-(4-(trifluoromethyl)phenyl)diazene (8(6))

This intermediate was prepared from 10 by a procedure similar to that used for preparation of 7(6). A yellow solid of 8(6) was obtained in 76.8% yield. (400 MHz, CDCl$_3$, δ, TMS, ppm): 7.97 (4H, m, ArH ortho to −N=N−), 7.77 (2H, d, ArH ortho to CF$_3$), 7.00 (2H, d, ArH ortho to OCH$_2$), 4.09 (2H, t, OCH$_2$), 3.41 (2H, t, CH$_2$Br), 1.85−1.92 (4H, d, [CH$_2$]$_2$) and 1.51−1.56 (4H, t, [CH$_2$]$_2$).

2.3.5. (E)-1-(4-(12-bromododecyloxy)phenyl)-2-phenyldiazene (7(12))

This intermediate was prepared from 9 by a procedure similar to that used for preparation of 7(6). 1,12-dibromododecane was used instead of 1,6-dibromohexane. A light yellow solid of 7(12) was obtained in 67.5% yield. ^{1}H NMR (400 MHz, CDCl$_3$, δ, TMS, ppm): 7.92 (4H, m, ArH ortho to −N=N−), 7.53 (3H, d, ArH meta and para

to −N=N−), 7.00 (2H, d, ArH ortho to OCH₂), 4.06 (2H, t, OCH₂), 3.43 (2H, t, CH₂Br), 1.79−1.88 (4H, m, OCH₂CH₂ and CH₂CH₂Br) and 1.24−1.47 (16H, m, [CH₂]₈).

2.3.6. (E)-1-(4-(12-bromododecyloxy)phenyl)-2-(4-(trifluoromethyl)phenyl)diazene (**8**(12))

This intermediate was prepared from **10** by a procedure similar to that used for preparation of **7**(6). 1,12-dibromododecane was used instead of 1,6-dibromohexane. A yellow solid of **8**(12) was obtained in 63.4% yield. ¹H NMR (300 MHz, CDCl₃, δ, TMS, ppm): 7.97 (4H, m, ArH ortho to −N=N−), 7.77 (2H, d, ArH ortho to CF₃), 7.00 (2H, d, ArH ortho to OCH₂), 4.07 (2H, t, OCH₂), 3.43 (2H, t, CH₂Br), 1.80−1.88 (4H, m, OCH₂CH₂ and CH₂CH₂Br) and 1.30−1.45 (16H, m, [CH₂]₈).

2.3.7. (E)-1-(4-(6-(4-iodophenoxy)hexyloxy)phenyl)-2-phenyldiazene (**5**(6))

In a 250 mL round-bottom flask equipped with a reflux condenser, 4-idophenol (1.1 g, 5 mmol), KOH (0.31 g, 5.5 mmol) and KI (0.25 g, 1.5 mmol) were dissolved in 100 mL of acetone/DMSO (9:1 by volume) mixture with stirring. To the reaction mixture was added of **7**(6) (1.80 g, 5 mmol) and the resultant mixture was refluxed for 24 h. The solid was removed by filtration and the filtrate was concentrated under reduced pressure. The mixture was washed by excess, dilute hydrochloric acid and extracted with chloroform for 3 times. The chloroform solution was then washed by saturated NaHCO₃ and NaCl solutions. The mixture was dried over 4.5 g of magnesium sulfate. The crude product was condensed and purified by column chromatography using a mixture of petroleum ether and ethyl acetate (5:1 by volume) as eluent. A light yellow solid of **5**(6) was obtained in 90.8% yield. ¹H NMR (400 MHz,

CDCl₃, δ, TMS, ppm): 7.94 (4H, m, ArH ortho to −N=N−), 7.49 (4H, m, ArH meta to −N=N− and ArH ortho to I), 7.44 (1H, t, ArH para to −N=N−), 7.00 (2H, d, ArH ortho to OCH₂), 6.67 (2H, d, ArH meta to I), 4.05 (2H, t, CH₂O), 3.93 (2H, t, CH₂O), 1.81 (4H, m, [CH₂]₂), 1.27−1.57 (4H, t, [CH₂]₂).

2.3.8. (E)-1-(4-(6-(4-iodophenoxy)hexyloxy)phenyl)-2-(4-(trifluoromethyl)phenyl)-diazene (**6**(6))

This intermediate was prepared from **8**(6) by a procedure similar to that used for preparation of **5**(6). A light yellow solid of **6**(6) was obtained in 80.5% yield. ¹H NMR (400 MHz, CDCl₃, δ, TMS, ppm): 7.97 (4H, m, ArH ortho to −N=N−), 7.77 (2H, d, ArH ortho to F₃C), 7.56 (2H, d, ArH ortho to I), 7.00 (2H, d, ArH ortho to OCH₂), 6.69 (2H, d, ArH meta to I), 4.09 (2H, t, OCH₂), 3.96 (2H, t, CH₂O), 1.54−1.89 (8H, m, [CH₂]₂).

2.3.9. (E)-1-(4-(12-(4-iodophenoxy)dodecyloxy)phenyl)-2-phenyldiazene (**5**(12))

This intermediate was prepared from **7**(12) by a procedure similar to that used for preparation of **5**(6). A light yellow solid of **5**(12) was obtained in 84.5% yield. ¹H NMR (400 MHz, CDCl₃, δ, TMS, ppm): 7.94 (4H, m, ArH ortho to −N=N−), 7.43−7.55 (5H, m, ArH meta and para to −N=N−, ArH ortho to I), 7.00 (2H, d, ArH ortho to OCH₂), 6.67 (2H, d, ArH meta to I), 4.06 (2H, t, OCH₂), 3.92 (2H, t, CH₂O), 1.71−1.86 (4H, m, [CH₂]₂), 1.30−1.50 (16H, t, [CH₂]₂).

2.3.10. (E)-1-(4-(12-(4-iodophenoxy)dodecyloxy)phenyl)-2-(4-(trifluoromethyl)phenyl)-diazene (**6**(12))

This intermediate was prepared from **8**(12) by a procedure similar to that used for preparation of **5**(6). A light yellow solid of **6**(12) was obtained in 88.6% yield. ¹H NMR (400 MHz, CDCl₃, δ, TMS,
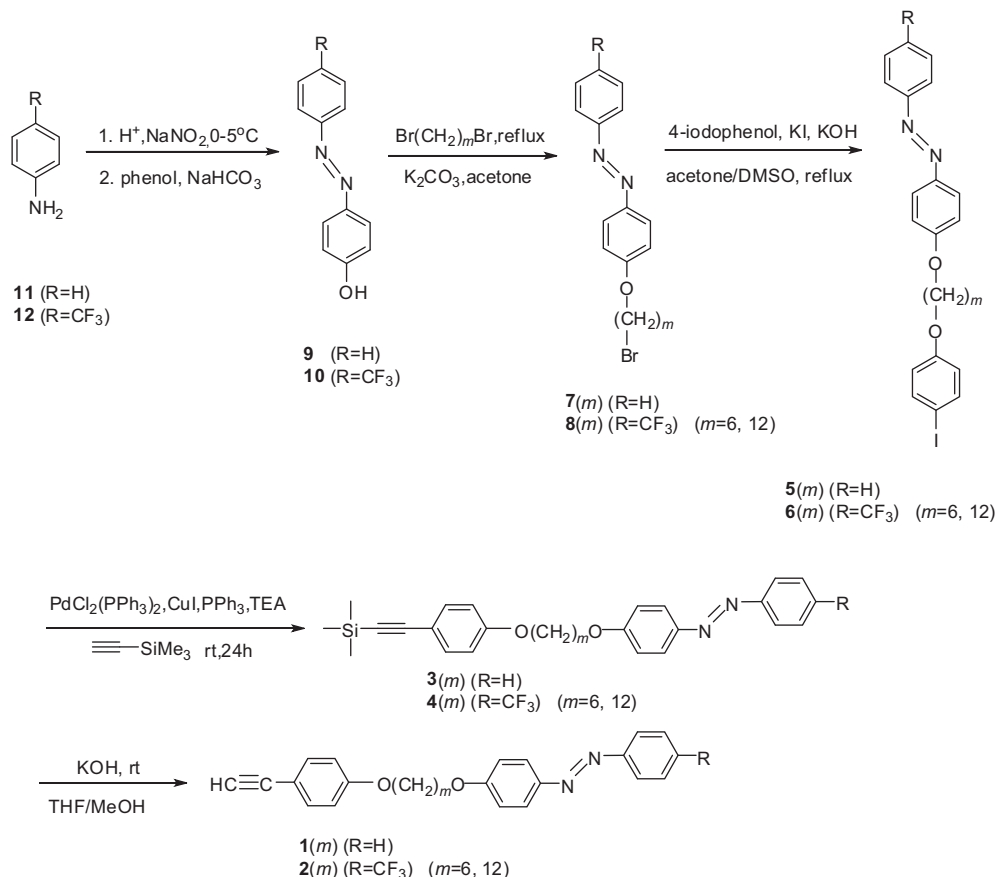
Scheme 1.

ppm): 7.97 (4H, m, ArH ortho to −N=N−), 7.77 (2H, d, ArH ortho to F$_3$C), 7.55 (2H, d, ArH ortho to I), 6.99 (2H, d, ArH ortho to OCH$_2$), 6.69 (2H, d, ArH meta to I), 4.07 (2H, t, OCH$_2$), 3.97 (2H, t, CH$_2$O), 1.50–1.90 (20H, m, [CH$_2$]$_2$).

2.3.11. (E)-1-phenyl-2-(4-(6-(4-((trimethylsilyl)ethynyl)phenoxy) hexyloxy)phenyl)-diazene (3(6))

In a 250 mL two-necked round-bottom flask were added PdCl$_2$(PPh$_3$)$_2$ (14 mg, 0.02 mmol), CuI (3.8 mg, 0.02 mmol), PPh$_3$ (10.5 mg, 0.04 mmol) and 15 mL THF solution of 5(6) (1.0 g, 2 mmol) under nitrogen. 25 mL TEA and 15 mL piperidine were injected to better dissolve the catalysts. After the catalysts were completely dissolved, trimethylsilylacetylene (0.24 g, 2.4 mmol) was injected into the flask and the mixture was stirred at room temperature for 12 h. The solid was removed by filtration and washed with diethyl ether. The filtrate was then concentrated by a rotary evaporator. The crude product was purified by column chromatography using a mixture of petroleum ether and ethyl acetate (20:1 by volume) as eluent. A light yellow solid of 3(6) was obtained in 92.2% yield. ^{1}H NMR (400 MHz, CDCl$_3$, δ, TMS, ppm): 7.93 (4H, m, ArH ortho to −N=N−), 7.38−7.51 (5H, m, ArH meta and para to −N=N−, ArH ortho to ≡), 7.00 (2H, d, ArH ortho to OCH$_2$), 6.83 (2H, d, ArH meta to ≡), 4.08 (2H, t, OCH$_2$), 3.97 (2H, t, CH$_2$O), 1.84 (4H, m, [CH$_2$]$_2$), 1.25−1.58 (4H, t, [CH$_2$]$_2$), 0.24 (9H, s, Si [CH$_3$]$_3$).

2.3.12. (E)-1-(4-(trifluoromethyl)phenyl)-2-(4-(6-(4-((trimethylsilyl)ethynyl)phenoxy)-hexyloxy)phenyl)diazene (4(6))

This intermediate was prepared from 6(6) by a procedure similar to that used for preparation of 3(6). A yellow solid of 4(6) was obtained in 91.4% yield. ^{1}H NMR (400 MHz, CDCl$_3$, δ, TMS, ppm): 7.97 (4H, m, ArH ortho to −N=N−), 7.74−7.77 (2H, d, ArH ortho to CF$_3$), 7.38−7.41 (2H, m, ArH ortho to ≡), 7.00 (2H, d, ArH ortho to OCH$_2$), 6.80 (2H, d, ArH meta to ≡), 4.11 (2H, t, OCH$_2$), 4.00 (2H, t, CH$_2$O), 1.85 (4H, m, [CH$_2$]$_2$), 1.25−1.58 (4H, t, [CH$_2$]$_2$), 0.24 (9H, s, Si[CH$_3$]$_3$).

2.3.13. (E)-1-phenyl-2-(4-(12-(4-((trimethylsilyl)ethynyl)phenoxy) dodecyloxy)phenyl)-diazene (3(12))

This intermediate was prepared from 5(12) by a procedure similar to that used for preparation of 3(6). A yellow solid of 3(12) was obtained in 83.5% yield. ^{1}H NMR (400 MHz, CDCl$_3$, δ, TMS, ppm): 7.94 (4H, m, ArH ortho to −N=N−), 7.37−7.53 (5H, m, ArH meta and para to −N=N−, ArH ortho to ≡), 7.00 (2H, d, ArH ortho to OCH$_2$), 6.82 (2H, d, ArH meta to ≡), 4.06 (2H, t, OCH$_2$), 3.96 (2H, t, CH$_2$O), 1.87 (4H, m, [CH$_2$]$_2$), 1.30−1.45 (16H, d, [CH$_2$]$_8$), 0.24 (9H, s, Si [CH$_3$]$_3$).

2.3.14. (E)-1-(4-(trifluoromethyl)phenyl)-2-(4-(12-(4-((trimethylsilyl)ethynyl)phenoxy)-dodecyloxy)phenyl)diazene (4(12))

This intermediate was prepared from 6(12) by a procedure similar to that used for preparation of 4(6). A yellow solid of 4(12) was obtained in 94.6% yield. ^{1}H NMR (400 MHz, CDCl$_3$, δ, TMS, ppm): 7.97 (4H, m, ArH ortho to −N=N−), 7.75−7.77 (2H, d, ArH ortho to CF$_3$), 7.37−7.40 (2H, m, ArH ortho to ≡), 6.99 (2H, d, ArH ortho to OCH$_2$), 6.80 (2H, d, ArH meta to ≡), 4.10 (2H, t, OCH$_2$), 4.00 (2H, t, CH$_2$O), 1.86 (4H, m, [CH$_2$]$_2$), 1.26−1.50 (16H, t, [CH$_2$]$_2$), 0.24 (9H, s, Si[CH$_3$]$_3$).

2.3.15. (E)-1-(4-(6-(4-ethynylphenoxy)hexyloxy)phenyl)-2-phenyldiazene (1(6))

In a 250 mL round-bottom flask were added 3(6) (0.94 g, 2 mmol), KOH (0.68 g, 12 mmol), 50 mL THF, and 50 mL methanol. The mixture was stirred at room temperature for 12 h and then

poured into 1000 mL of 1 M HCl solution. The mixture was extracted by DCM 3 times and the organic layers were collected. The solvents were removed under reduced pressure, and the crude product was purified by column chromatography using a mixture of petroleum ether and ethyl acetate (5:1 by volume) as eluent. A light yellow solid of 1(6) was obtained in 81.4% yield.

Characterization data: ^{1}H NMR (400 MHz, CDCl$_3$, δ, TMS, ppm): 7.92 (4H, m, ArH ortho to −N=N−), 7.40−7.51 (5H, m, ArH meta and para to −N=N−, ArH ortho to ≡), 7.00 (2H, d, ArH ortho to OCH$_2$), 6.81−6.83 (2H, d, ArH meta to ≡), 4.05 (2H, t, OCH$_2$), 3.97 (2H, t, CH$_2$O), 3.00 (1H, s, ≡CH), 1.81−1.84 (4H, m, [CH$_2$]$_2$), 1.25−1.60 (4H, t, [CH$_2$]$_2$). ^{13}C NMR (400 MHz, CDCl$_3$, δ, TMS, ppm): 161.6, 159.4 (aromatic carbons attached to −N=N−), 152.7, 148.9 (aromatic carbons attached to −O−), 133.6 (aromatic carbons ortho to ≡), 130.3 (aromatic carbon para to −N=N−), 129.0 (aromatic carbons meta to −N=N−), 124.7 and 122.5 (aromatic carbons ortho to −N=N−), 114.7, 114.4 and 113.9 (aromatic carbons ortho and para to −O−), 83.7 (≡C attached to benzene), 75.7 (≡C−H), 68.1 and 67.8 (carbons attached to −O−), 29.1 (OCH$_2$CH$_2$), 25.8 (CH$_2$). IR (KBr), ν (cm^{-1}): 3285 (HC≡C), 2949 and 2875 (H−CH), 1400 (N= N). Calcd for C$_{26}$H$_{26}$N$_2$O$_2$ (398.5): C, 78.36; H, 6.58; N, 7.03. Found: C, 78.14; H, 6.63; N, 7.11.

2.3.16. (E)-1-(4-(6-(4-ethynylphenoxy)hexyloxy)phenyl)-2-(4-(trifluoromethyl)phenyl)-diazene (2(6))

This monomer was prepared from 4(6) by a procedure similar to that used for preparation of 1(6). A yellow solid of 2(6) was obtained in 88.5% yield.

Characterization data: ^{1}H NMR (400 MHz, CDCl$_3$, δ, TMS, ppm): 7.95 (4H, m, ArH ortho to −N=N−), 7.72−7.75 (2H, d, ArH ortho to CF$_3$), 7.41 (2H, m, ArH ortho to ≡), 7.00 (2H, d, ArH ortho to OCH$_2$), 6.80 (2H, d, ArH meta to ≡), 4.07 (2H, t, OCH$_2$), 3.98 (2H, t, CH$_2$O), 3.00 (1H, s, ≡CH), 1.85 (4H, m, [CH$_2$]$_2$), 1.25−1.57 (4H, t, [CH$_2$]$_2$). ^{13}C NMR (400 MHz, CDCl$_3$, δ, TMS, ppm): 161.6, 159.4 (aromatic carbons attached to −N=N−), 152.7, 148.9 (aromatic carbons attached to −O−), 133.6 (aromatic carbons ortho to ≡), 131.5 (aromatic carbon para to −N=N−), 126.3 (aromatic carbons meta to −N=N−), 124.7 and 122.5 (aromatic carbons ortho to −N=N−), 114.7, 114.4 and 113.9 (aromatic carbons ortho and para to −O−), 83.7 (≡C attached to benzene), 75.7 (≡C−H), 68.1 and 67.8 (carbons attached to −O−), 29.1 (OCH$_2$CH$_2$), 25.8 (CH$_2$). IR (KBr), ν (cm^{-1}): 3285 (HC≡C), 2949 and 2875 (H−CH), 1400 (N=N). Calcd for C$_{27}$H$_{25}$F$_3$N$_2$O$_2$ (466.49): C, 69.52; H, 5.40; N, 6.01. Found: C, 69.05; H, 5.34; N, 6.08.

2.3.17. (E)-1-(4-(12-(4-ethynylphenoxy)dodecyloxy)phenyl)-2-phenyldiazene (1(12))

This monomer was prepared from 3(12) by a procedure similar to that used for preparation of 1(6). A light yellow solid of 1(12) was obtained in 98.0% yield.

Characterization data: ^{1}H NMR (400 MHz, CDCl$_3$, δ, TMS, ppm): 7.92 (4H, m, ArH ortho to −N=N−), 7.39−7.51 (5H, m, ArH meta and para to −N=N−, ArH ortho to ≡), 7.00 (2H, d, ArH ortho to OCH$_2$), 6.82 (2H, d, ArH meta to ≡), 4.04 (2H, t, OCH$_2$), 3.97 (2H, t, CH$_2$O), 3.00 (1H, s, ≡CH), 1.75−1.84 (4H, m, [CH$_2$]$_2$), 1.25−1.47 (16H, t, [CH$_2$]$_8$). ^{13}C NMR (400 MHz, CDCl$_3$, δ, TMS, ppm): 161.6, 159.4 (aromatic carbons attached to −N=N−), 152.7, 148.9 (aromatic carbons attached to −O−), 133.6 (aromatic carbons ortho to ≡), 130.3 (aromatic carbon para to −N=N−), 129.0 (aromatic carbons meta to −N=N−), 124.7 and 122.5 (aromatic carbons ortho to −N= N−), 114.7, 114.4 and 113.9 (aromatic carbons ortho and para to −O−), 83.7 (≡C attached to benzene), 75.7 (≡C−H), 68.1 and 67.8 (carbons attached to −O−), 29.1 (OCH$_2$CH$_2$), 25.8 (CH$_2$). IR (KBr), ν (cm^{-1}): 3285 (HC≡C), 2949 and 2875 (H−CH), 1400 (N=N). Calcd for C$_{32}$H$_{38}$F$_3$N$_2$O$_2$ (482.66): C, 79.63; H, 7.94; N, 5.80. Found: C, 79.42; H, 7.96; N, 5.92.

2.3.18. (E)-1-(4-(12-(4-ethynylphenoxy)dodecyloxy)phenyl)-2-(4-(trifluoromethyl)-phenyl)diazene (2(12))

This monomer was prepared from 4(12) by a procedure similar to that used for preparation of 1(6). A light yellow solid of 2(12) was obtained in 94.2% yield.

Characterization data: ^{1}H NMR (400 MHz, CDCl$_3$, δ, TMS, ppm): 7.95 (4H, m, ArH ortho to −N=N−), 7.72–7.75 (2H, d, ArH ortho to CF$_3$), 7.41 (2H, m, ArH ortho to ≡), 7.00 (2H, d, ArH ortho to OCH$_2$), 6.80 (2H, d, ArH meta to ≡), 4.07 (2H, t, OCH$_2$), 3.98 (2H, t, CH$_2$O), 3.00 (1H, s, ≡CH), 1.85 (4H, m, [CH$_2$]$_2$), 1.25–1.57 (4H, t, [CH$_2$]$_2$). ^{13}C NMR (400 MHz, CDCl$_3$, δ, TMS, ppm): 161.6, 159.4 (aromatic carbons attached to −N=N−), 152.7, 148.9 (aromatic carbons attached to −O−), 133.6 (aromatic carbons ortho to ≡), 131.5 (aromatic carbon para to −N=N−), 126.3 (aromatic carbons meta to −N=N−), 124.7 and 122.5 (aromatic carbons ortho to −N=N−), 114.7, 114.4 and 113.9 (aromatic carbons ortho and para to −O−), 83.7 (≡C attached to benzene), 75.7 (≡C−H), 68.1 and 67.8 (carbons attached to −O−), 29.1 (OCH$_2$CH$_2$), 25.8 (CH$_2$). IR (KBr), ν (cm^{-1}): 3285 (HC≡C), 2949 and 2875 (H−CH), 1400 (N=N). HRMS (CI): m/z 551.2859 [(M + 1)$^+$, calcd 551.2807, see Figure S1].

2.4. Polymerization preparation

All the phenylacetylene derivatives polymerizations and manipulations were carried out under dry nitrogen using Schlenk techniques in a vacuum-line system except for the purification of the polymers, which was done in air. The synthetic route is shown as Scheme 2 and typical experimental procedures for polymerization of 1(6) are given below as an example.

In a 20 mL baked Schlenk tube with a side arm was added 99 mg (0.25 mmol) of monomer 1(6). The tube was evacuated under vacuum and flushed with dry nitrogen three times through the side arm. Then 1.5 mL of THF was injected into the tube to dissolve the monomer. The catalyst solution was prepared in another tube by dissolving [Rh(nbd)Cl]$_2$ or [Rh(cod)Cl]$_2$ in 1 mL of THF with one drop of TEA added. After aging for 15 min, the catalyst solution was

transferred to the monomer solution using a hypodermic syringe. The mixture was stirred at room temperature under nitrogen for 24 h and was then diluted with 10 mL of THF and added dropwise to a 500 mL methanol through a cotton filter under stirring. The precipitate was allowed to stand for 24 h and then filtered with a Gooch crucible. The polymer was washed with methanol for three times and then dried in a vacuum oven at 25 °C to a constant weight.

2.4.1. Characterization data for P1(6)

Brown powdery solid; yield 84.7%. M_w: 44,700; M_w/M_n: 1.93 (GPC, polystyrene calibration; Table 1, no. 2). ^{1}H NMR (400 MHz, CDCl$_3$, δ, TMS, ppm): 7.80–7.90 (ArH ortho to −N=N−), 7.39–7.50 (ArH meta and para to −N=N−), 6.36, 6.60, 7.00 (ArH ortho to OCH$_2$, ArH ortho and meta to =), 5.80 (H−C=C), 3.70–4.06 (OCH$_2$), 1.26–1.84 (CH$_2$]$_2$). ^{13}C NMR (400 MHz, CDCl$_3$, δ, TMS, ppm): 161.6, 159.4 (aromatic carbons attached to −N=N−), 152.7, 148.9 (aromatic carbons attached to −O−), 130.3 (aromatic carbon para to −N=N−), 129.0 (aromatic carbons meta to −N=N−), 124.7 and 122.5 (aromatic carbons ortho to −N=N−), 114.7, 114.4 and 113.9 (aromatic carbons ortho and para to −O−), 68.1 and 67.8 (carbons attached to −O−), 29.1 (OCH$_2$CH$_2$), 25.8 (CH$_2$). IR (KBr), ν (cm^{-1}): 2949 and 2875 (H−CH), 1400 (N=N).

2.4.2. Characterization data for P1(12)

Brown powdery solid; yield 85.5%. M_w: 76,600; M_w/M_n: 1.79 (GPC, polystyrene calibration; Table 1, no. 7). ^{1}H NMR (400 MHz, CDCl$_3$, δ, TMS, ppm): 7.84–7.92 (ArH ortho to −N=N−), 7.41–7.52 (ArH meta and para to −N=N−), 6.36, 6.60, 7.00 (ArH ortho to OCH$_2$, ArH ortho and meta to =), 5.80 (H−C=C), 3.87–4.03 (OCH$_2$),

Scheme 2.

Table 1
Polymerization of monomers 1(6), 2(6), 1(12), and 2(12).[a]

No	Catalyst[b]	[M]$_0$ (M)	[Cat.] (mM)	Yield (%)	M_w[c]	M_w/M_n[c]
Monomer 1(6)						
1	[Rh(cod)Cl]$_2$	0.10	2.00	55.4	33,700	1.59
2	[Rh(nbd)Cl]$_2$	0.20	8.50	84.7	44,700	1.92
3	[Rh(nbd)Cl]$_2$	0.10	2.50	65.4	60,600	1.60
Monomer 2(6)						
4	[Rh(nbd)Cl]$_2$	0.10	6.00	97.4	42,300	1.58
5	[Rh(nbd)Cl]$_2$	0.10	2.00	84.2	66,500	1.90
6	[Rh(cod)Cl]$_2$	0.10	2.00	61.1	45,500	1.69
Monomer 1(12)						
7	[Rh(nbd)Cl]$_2$	0.05	2.50	85.5	76,600	1.79
8	[Rh(nbd)Cl]$_2$	0.10	6.00	89.0	41,300	1.47
9	[Rh(nbd)Cl]$_2$	0.10	2.00	79.3	92,200	1.90
10	[Rh(cod)Cl]$_2$	0.10	2.00	66.1	57,700	1.90
Monomer 2(12)						
11	[Rh(nbd)Cl]$_2$	0.10	2.00	85.1	86,600	1.95
12	[Rh(cod)Cl]$_2$	0.10	2.00	60.7	66,300	1.70

[a] Carried out at room temperature in an atmosphere of dry nitrogen for 24 h in THF/Et$_3$N.
[b] Abbreviations: nbd = 2.5-norborndiene and cod = 1,5-cyclooctadiene.
[c] Determined by gel permeation chromatograph (GPC) in THF on the basis of a polystyrene calibration.
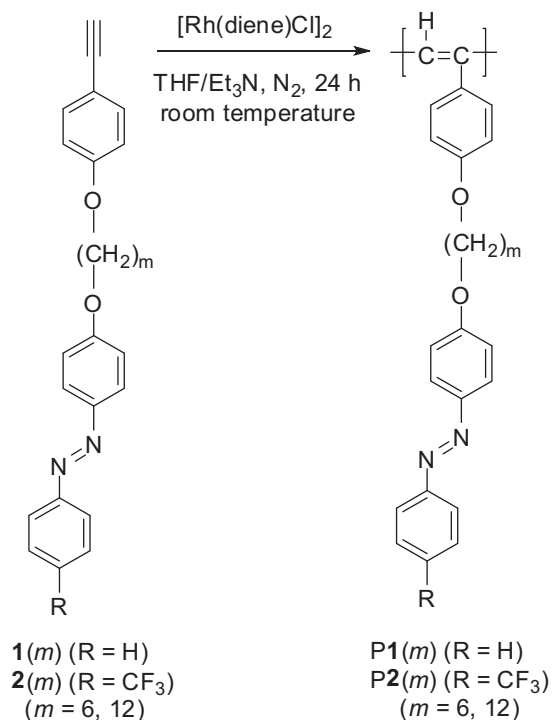
1.25−1.81 (CH$_2$]$_2$). ^{13}C NMR (400 MHz, CDCl$_3$, δ, TMS, ppm): 161.6, 159.4 (aromatic carbons attached to −N=N−), 152.7, 148.9 (aromatic carbons attached to −O−), 130.3 (aromatic carbon para to −N=N−), 129.0 (aromatic carbons meta to −N=N−), 124.7 and 122.5 (aromatic carbons ortho to −N=N−), 114.7, 114.4 and 113.9 (aromatic carbons ortho and para to −O−), 68.1 and 67.8 (carbons attached to −O−), 29.1 (OCH$_2$CH$_2$), 25.8 (CH$_2$). IR (KBr), ν (cm^{-1}): 2949 and 2875 (H−CH), 1400 (N=N).

2.4.3. Characterization data for P2(6)

Dark brown powdery solid; yield 84.2%. M_w: 66,500; M_w/M_n: 1.90 (GPC, polystyrene calibration; Table 1, no. 5). ^{1}H NMR (400 MHz, CDCl$_3$, δ, TMS, ppm): 7.78−7.96 (ArH ortho to −N=N−), 7.60−7.65 (ArH ortho to CF$_3$), 6.36, 6.60, 7.00 (ArH ortho to OCH$_2$, ArH ortho and meta to =), 5.80 (H−C=C), 3.70−4.06 (OCH$_2$), 1.26−1.84 (CH$_2$]$_2$). ^{13}C NMR (400 MHz, CDCl$_3$, δ, TMS, ppm): 161.6, 159.4 (aromatic carbons attached to −N=N−), 152.7, 148.9 (aromatic carbons attached to −O−), 130.3 (aromatic carbon para to −N=N−), 129.0 (aromatic carbons meta to −N=N−), 124.7 and 122.5 (aromatic carbons ortho to −N=N−), 114.7, 114.4 and 113.9 (aromatic carbons ortho and para to −O−), 68.1 and 67.8 (carbons attached to −O−), 29.1 (OCH$_2$CH$_2$), 25.8 (CH$_2$). IR (KBr), ν (cm^{-1}): 2949 and 2875 (H−CH), 1400 (N=N).

2.4.4. Characterization data for P2(12)

Dark brown powdery solid; yield 85.1%. M_w: 86,600; M_w/M_n: 1.95 (GPC, polystyrene calibration; Table 1, no. 11). ^{1}H NMR (400 MHz, CDCl$_3$, δ, TMS, ppm): 7.88−7.95 (ArH ortho to −N=N−), 7.74−7.76 (ArH ortho to CF$_3$), 6.36, 6.60, 7.00 (ArH ortho to OCH$_2$, ArH ortho and meta to =), 5.80 (H−C=C), 3.95−4.06 (OCH$_2$), 1.26−1.84 (CH$_2$]$_2$). ^{13}C NMR (400 MHz, CDCl$_3$, δ, TMS, ppm): 161.6, 159.4 (aromatic carbons attached to −N=N−), 152.7, 148.9 (aromatic carbons attached to −O−), 130.3 (aromatic carbon para to −N=N−), 129.0 (aromatic carbons meta to −N=N−), 124.7 and 122.5 (aromatic carbons ortho to −N=N−), 114.7, 114.4 and 113.9 (aromatic carbons ortho and para to −O−), 68.1 and 67.8 (carbons attached to −O−), 29.1 (OCH$_2$CH$_2$), 25.8 (CH$_2$). IR (KBr), ν (cm^{-1}): 2949 and 2875 (H−CH), 1400 (N=N).

3. Results and discussion

3.1. Polymer synthesis

By linking azobenzene to the phenyl ring through flexible spacers of six carbon atoms (1(6) and 2(6)) and twelve carbon atoms (1(12) and 2(12)), we obtained four azobenzene-containing phenylacetylene derivatives. These monomers were prepared through multi-step reactions shown in Scheme 1. All the reactions proceeded smoothly, and the desired monomers were isolated in satisfactory yields (∼81−98%). All of the intermediates and monomers were characterized by standard spectroscopic methods, from which satisfactory analysis data were obtained (see Experimental section for details).

To transform the monomers to polymers, we tried to use organorhodium complexes [Rh(diene)Cl]$_2$, which are widely used as effective catalysts to polymerize phenylacetylene derivatives. We first attempted to use [Rh(cod)Cl]$_2$ to polymerize monomer 1(6) in a THF/TEA mixture. The result was, however, not very satisfactory: polymer P1(6) was obtained in a yield of ∼55.4%, which was lower in comparison with the analogous polymerizations of phenylacetylene-based monomers, although the molecular weight was moderate (M_w ∼ 33,700, see Table 1, no. 1). Then we turned to catalyst [Rh(nbd)Cl]$_2$. Delightfully, the polymerization reaction gave a better result, affording a polymer in a higher yield of ∼84.7% with a higher M_w value of ∼44,700 (see Table 1, no. 2). All the other

monomers were readily polymerized by [Rh(nbd)Cl]$_2$ and [Rh(cod)Cl]$_2$ in a THF/TEA mixture. These polymerizations proceeded well in THF and produced polymers with high M_w value and accepted yield of ∼55.4−97.4% (see Table 1).

3.2. Structural characterization

The obtained polymers were characterized with multiple spectroscopic methods. All the polymers gave satisfactory analysis data corresponding to their expected molecular structures (see Experimental section for details). An example of the IR spectrum of P1(6) is shown in Fig. 1; the spectrum of its monomer 1(6) is also given in the same figure for comparison. The monomer exhibits absorption band at 3285 cm^{-1}, which is ascribed to ≡CH stretching vibrations. The band completely disappears in the spectrum of P1(6), indicating that the acetylene triple bond of 1(6) has been fully consumed by the rhodium-catalyzed polymerization reaction.

NMR spectroscopy is an effective method of characterizing the polymer structures. ^{1}H NMR spectra of polymer P1(6) and its monomer 1(6) are shown in Fig. 2. As can be seen from the ^{1}H NMR spectrum of P1(6), there is no resonance peak at δ ∼ 3.00, which is associated with the acetylene proton (Fig. 2B). A new peak associated with the resonance of olefinic protons appears at δ ∼ 5.80. The polymerization has thus transformed the acetylenic triple bond of 1(6) to olefinic double bond of P1(6). This accordingly causes upfield-shift in the resonance peaks of the phenyl protons, now occurring at δ 6.60 and 6.36 (Fig. 2B, peaks b and c).

The ^{13}C NMR spectra of polymer P1(6) and its monomer 1(6) are shown in Fig. 3. The acetylene carbon atoms of 1(6) resonate at δ 83.7 and 75.7, which completely disappear in the spectrum of P1(6). The resonance peaks of the polyene backbone carbon atoms of P1(6) are not distinguishable, probably because the polyene backbone are buried in the long side groups. Like the IR spectra, the NMR spectra duly confirm that the triple bond of the monomer has been consumed by the polymerization reaction, and the expected azobenzene-containing PPAs have been successfully derived.

3.3. Photoisomerization behaviors

UV−vis spectroscope was used to monitor the photoisomerization behaviors of the obtained polymers. The absorption spectra of the pristine polymers in THF solution show a strong band
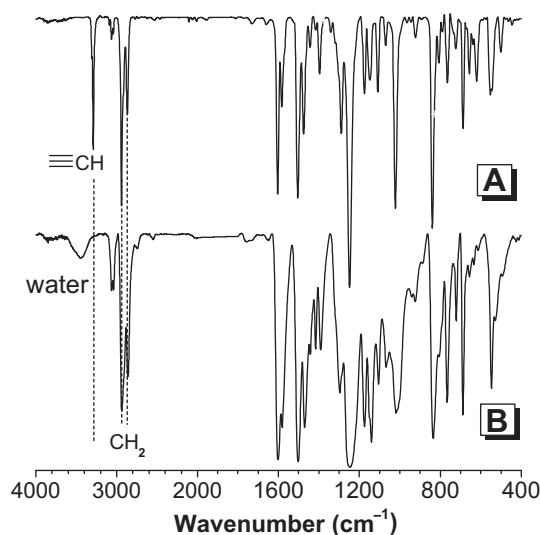

Fig. 1. FT-IR spectra of (A) monomer 1(6) and (B) its polymer P1(6) (sample from Table 1, no. 2).
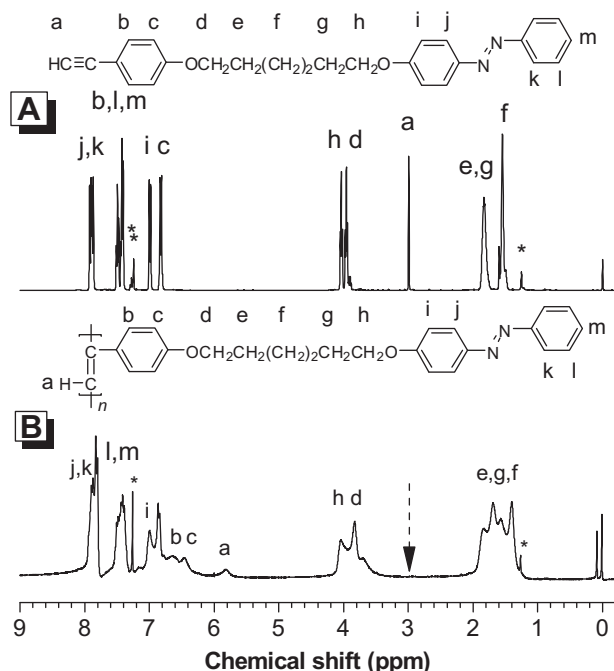
Fig. 2. ^{1}H NMR spectra of (A) **1**(6) and (B) its polymer P**1**(6) (sample from Table 1, no. 2) in chloroform-d. The solvent peaks are marked with asterisks.

at round 350 nm and weak broad tail at wavelengths longer than 400 nm (Fig. 4), which can be readily assigned by comparing with the absorption spectra of their monomers. The spectrum of **1**(6) is also given in Fig. 4 as a standard. The strong band of **1**(6) at round 350 nm is ascribed to the $\pi-\pi^*$ transition of the *trans*-form of azobenzene moieties. The polymers all exhibit an identical absorption band in the same wavelength region, indicating the pristine polymers take trans-configuration in THF solution. From the magnified spectra shown in the inset of Fig. 4, it can be seen that the absorption intensity of P**1**(6) at wavelengths longer than 400 nm is stronger than its monomer **1**(6). The weaker band of **1**(6)
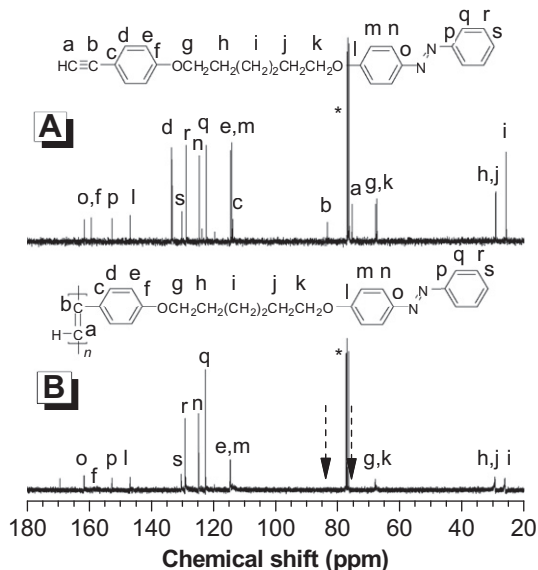

Fig. 3. ^{13}C NMR spectra of (A) **1**(6) and (B) its polymer P**1**(6) (sample from Table 1, no. 2) in chloroform-d. The solvent peaks are marked with asterisks.
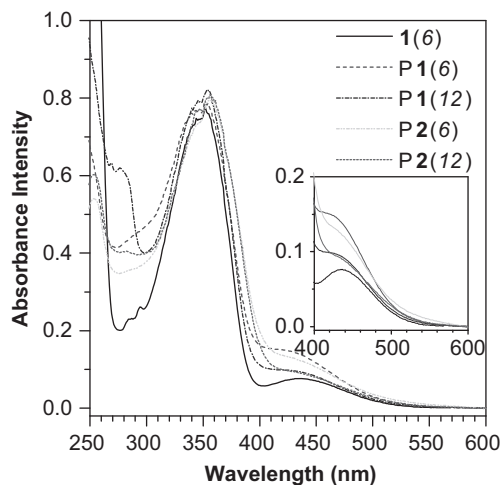

Fig. 4. Absorption spectra of polymers P**1**(6) (sample from Table 1, no. 2), P**1**(12) (Table 1, no. 7), P**2**(6) (Table 1, no. 5), P**2**(12) (Table 1, no. 11) and monomer **1**(6) in THF at room temperature. The concentration of solution is 5×10^{-5} M.

at around 440 nm is due to n−π* transition of the azobenzene pendants and the stronger absorption of P**1**(6) in the long wavelength region is evidently corresponding to the absorption of its polyene backbone.

Under proper ultraviolet irradiation, azobenzene compounds undergo isomerization from *trans*- to *cis*-forms, which is referred as photoisomerization. To examine the photoisomerization behavior of the polymers, we monitored the changes in absorption features of the monomers and their polymers in proper solutions by recording at different time intervals until *cis*-rich photostationary state was reached. Fig. 5 displays the recorded photoisomerization behavior of P**1**(6). After irradiation with 365 nm UV light (8 W), the absorption band at around 350 nm decreased continuously, while the absorption intensity at around 440 nm increased gradually. Furthermore, two isosbestic points at 313 and 408 nm were observed. The change of the absorption bands induced by UV irradiation is indicative of the photoisomerization of polymers carrying azobenzene pendants from the *trans* to the *cis* form. UV−vis absorption changes of the monomers and other azobenzene-containing polymers were also recorded under

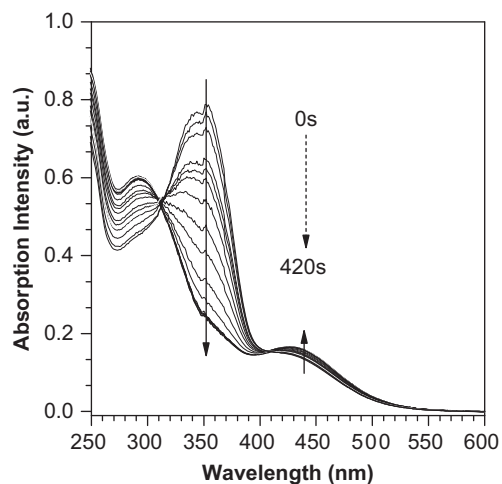**Fig. 5.** UV−vis absorption changes of P**1**(6) (sample from Table 1, no. 2) under different time interval during the irradiation time with 365 nm UV light (8 W) in THF at room temperature. The concentration of solution is 5×10^{-5} M.

different time interval during the irradiation time with 365 nm UV light in THF, and the results are shown in Figures S2–S8.

The kinetics of *trans−cis* photoisomerization of polymers P1(6), P1(12), P2(6), P2(12) and monomers 1(6) and 1(12) in THF solution were evaluated by analyzing the absorbance of the $\pi−\pi^*$ transition of the *trans*-form of azobenzene. The first-order rate constant was determined by the formula (1).

$$-k_e t = \ln[(A_\infty - A_t)/(A_\infty - A_0)] \qquad (1)$$

where k_e and t are the rate constant of photoisomerization and the time of UV-light irradiation, and A_0, A_t, and A_∞ represent the absorbance at around 350 nm at the time of beginning, time t, and time infinite, respectively. Extracting experimental data from Fig. 5, the photoisomerization kinetics of these polymers and monomers are plotted in Fig. 6. All the polymers and the monomers display linear relationship between the natural logarithm of specific absorbance difference, or $(A_\infty - A_t)/(A_\infty - A_0)$ and UV-light illumination time. The linear dependence suggests that the photoisomerization of the polymers as well as the monomers follows the first-order kinetics, and the rigid polyene backbone has not changed the basic kinetics of the azobenzene moieties attaching to it via a flexible alkyl spacer.

But the polymer backbone has inevitably influenced the rate of photoisomerization. Deduced from Fig. 6, the photoisomerization rate constant, k_e, of polymers P1(6), P1(12), P2(6), and P2(12) is 0.013, 0.014, 0.015, and 0.017 s^{-1}, respectively. The average rate constant of the polymers is about 0.015 s^{-1}, which is lower than the literature value derived from experiments conducted under similar conditions. When compared with monomers 1(6) and 1(12) (0.022 s^{-1}), the average k_e of the polymers decreases by nearly 32%. This is reasonable that the *trans*-to-*cis* transition resistance existed in small molecules is lower than that in macromolecules.

We also studied the photoisomerization behavior of four polymers as film state. Fig. 7 shows the UV spectra of P2(12) film under UV irradiation and further heating for a certain time. It is clear that the isomerization of polymer film from *trans*- to *cis*-rich photostationary state is 4.3 times slower than the corresponding polymer solution (see Figure S8). We can also noted that, by heating the film at 90 °C for 5 min, the *cis*-rich P2(12) was largely transformed to *trans*-form. Therefore, it is understandable that the azobenzene
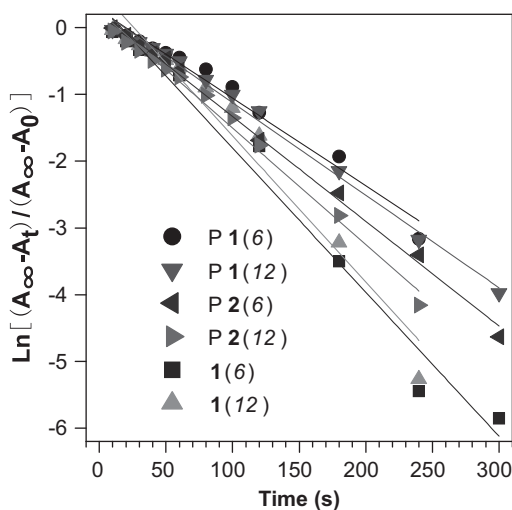

Fig. 7. UV−vis absorption changes of P2(12) (sample from Table 1, no. 11) film during the irradiation with UV light (365 nm, 8 W) at room temperature (rt) and further heating at 90 °C for 5 min. The irradiation time is marked as numeral.

moiety must have taken *trans*-form when the polymer film was quenched from its isotropic state. Indeed, only the *trans*-form azobenzene is regarded as a kind of mesogen to form liquid crystal. The UV spectra of polymer films of P1(6), P1(12) and P2(6) under UV irradiation and heating were also tested, and the effect of irradiation time on absorbance intensity changes at 354 nm is shown in Fig. 8. Despite their structural differences, four polyacetylenes adopted similar isomerization behaviors due to the fact that the azobenzene moieties were equally suppressed so as to undergo identically slow isomerization.

3.4. Thermal stability

Azobenzene is a widely used mesogen in the construction of thermotropic liquid-crystalline polymers, and heating is necessary for the generation of the mesophases. Therefore, the thermal stability of the polymers is one of the key parameters and we evaluated the thermal stability of P1(6), P2(6), P1(12), and P2(12) by thermal gravimetric analysis (TGA) technique. The recorded thermograms for the polymers are shown in Fig. 9; the T_d values for P1(6), P2(6), P1(12), and P2(12) are picked up from the TGA curves

Fig. 6. First-order *trans−cis* isomerization kinetic of polymers P1(6) (sample from Table 1, no. 2), P1(12) (Table 1, no. 7), P2(6) (Table 1, no. 5), P2(12) (Table 1, no. 11) and monomers 1(6) and 1(12) in THF solution under different time interval at room temperature. The concentration of solution is 5×10^{-5} M.
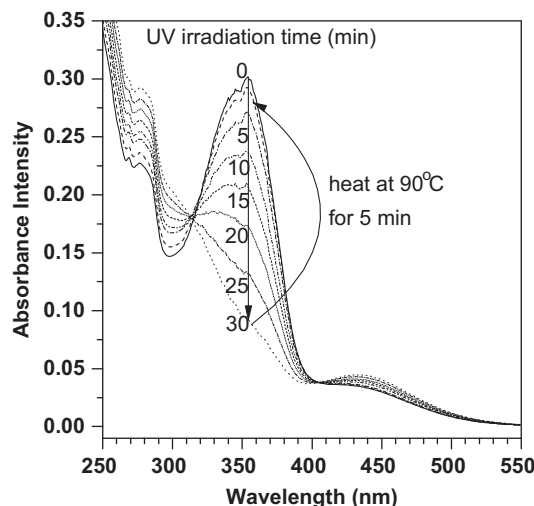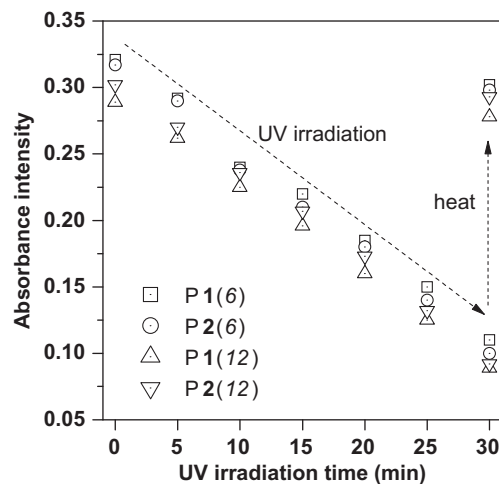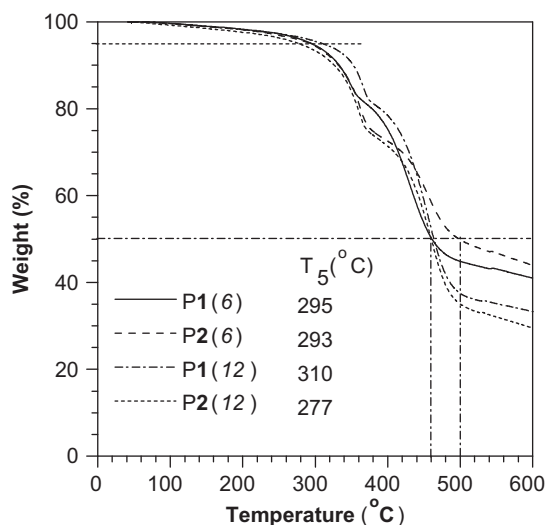

Fig. 8. Absorbance intensity changes at 354 nm of polymer films of P1(6) (sample from Table 1, no. 2), P1(12) (Table 1, no. 7), P2(6) (Table 1, no. 5), P2(12) (Table 1, no. 11) under UV irradiation (365 nm, 8 W) at rt and further heating at 90 °C for 5 min.
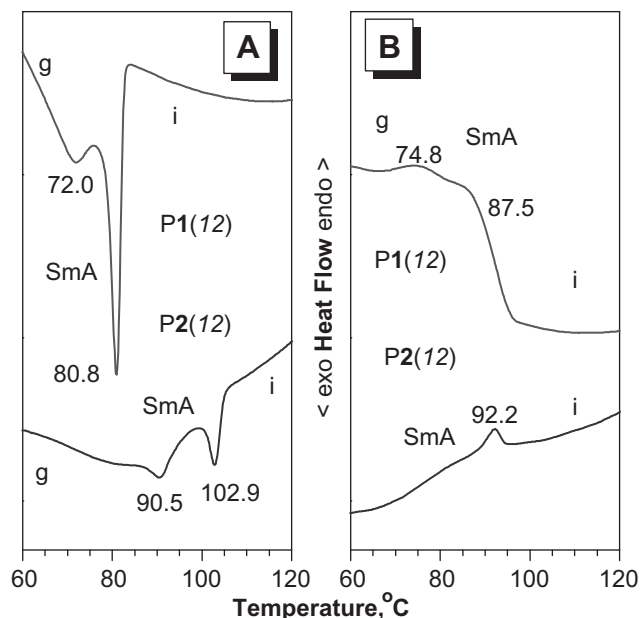
Fig. 9. TGA thermograms of P**1**(6) (sample from Table 1, no. 2), P**1**(12) (Table 1, no. 7), P**2**(6) (Table 1, no. 5), and P**2**(12) (Table 1, no. 11) measured under nitrogen at a heating rate of 20 °C/min.

Fig. 11. DSC thermograms of P**1**(12) (Table 1, no. 7) and P**2**(12) (Table 1, no. 11) recorded under nitrogen during the (A) first cooling and (B) second heating scans at a scan rate of 10 °C/min.

as 295, 293, 310, and 277 °C, respectively. These data indicate that these azobenzene-containing polymers have higher thermal stability than their parent polymer, or poly(phenylacetylene) (PPA), which shows a decomposition temperature (T_d, defined as the temperature at which the polymer loses 5% of its original weight) of 225 °C [85]. The improved thermal stability can be ascribed to the "jacket effect" of the bulky azobenzene pendants attached to the PPA backbone [4–6,86–89]. In comparison with the azobenzene-containing polyacrylates, the increase in decomposition temperature is more pronounced. For example, Zhang and colleagues recently reported a series of polymethacrylate-based photo-responsive side-chain liquid-crystalline polymers with azobenzene mesogen; the decomposition temperatures of these polymers are all lower than 280 °C [32]. The elevated decomposition temperature of the obtained azobenzene-containing polyphenylacetylenes is desirable because high thermal stability is required by many high-tech applications.

3.5. Liquid crystallinity

After checking the thermal stabilities of the polymers, we proceeded to study their liquid crystallinity. Polarized optical microscope (POM) was used to examine the mesomorphic behaviors of these azobenzene-containing polymers. Fig. 10 shows the POM microphotographs of the textures of P**1**(12) and P**2**(12) recorded in the heating–cooling cycles. When P**2**(12) was cooled from its isotropic state, very small bâtonnets emerged from the homotropic dark background, forming an anisotropic mesomorphic texture. This indicates that P**2**(12) is a liquid-crystalline polymer. The texture contains tiny bands, whose directors are perpendicular to the long axes of the bâtonnets. Such in-domain bands are frequently observed during the formation of the focal-conic textures in liquid-crystalline polyacetylenes [13–18], suggesting that the mesophase of P**2**(12) is in a nature smectic A phase. In an attempt to grow bâtonnets to bigger focal-conic texture, after cooling P**2**(12) to 91.7 °C, we annealed the sample at the same temperature and observed fan-shaped patterns with a diameter of 35 μm at the annealing time of 30 min (Fig. 10B). When P**1**(12) was cooled from its melting state, many anisotropic entities emerged from the background (Fig. 10C). However, the development of these tiny entities into a typical SmA texture was difficult. For both P**1**(6)
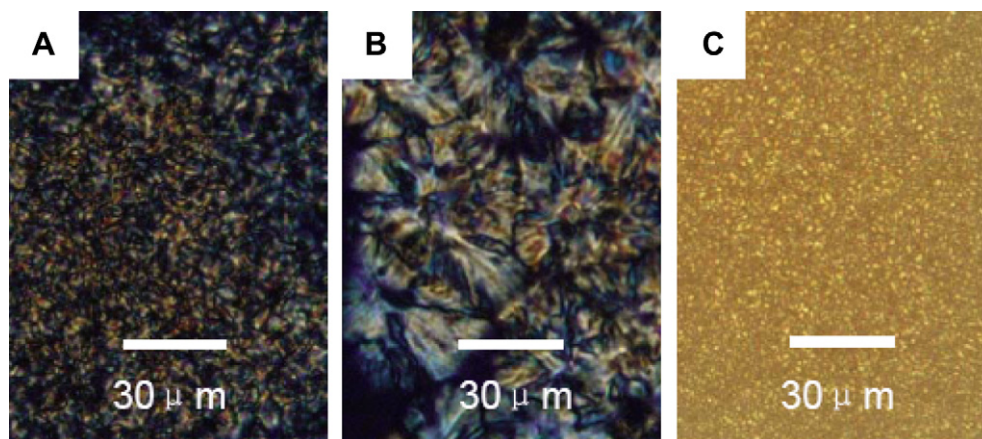

Fig. 10. Mesomorphic textures observed on cooling (A) P**2**(12) to 91.7 °C, (B) P**2**(12) to 91.7 °C and followed by annealing for 30 min, (C) P**1**(12) to 74.5 °C from their isotropic states at a cooling rate of 3 °C/min.

Table 2
Thermal properties of polymers P1(6), P2(6), P1(12) and P2(12).[a]

Polymer	T, °C	
	Cooling	Heating
P1(6)	i 102.9 k(g)	k(g) 108.1 i
P2(6)	i 113.3 k(g)	k(g) 121.3 i
P1(12)	i 80.8 SmA 72.0 k(g)	k(g) 74.8 SmA 87.5 i
P2(12)	i 102.9 SmA 90.5 k(g)	k(g) 92.2 SmA 105.4 i

[a] Data taken from the DSC thermograms recorded under nitrogen in the first cooling and second heating scans; abbreviations: k = crystalline state, g = glassy state, SmA = smectic A phase, i = isotropic liquid.

and P2(6), the POM observation gave a disappointing result that they were not liquid crystalline. This is probably due to the shorter flexible spacer and the stiff polymer backbone, which hinder the alignment of the azobenzene mesogen. In contrast, the two monomers 1(12) and 2(12) both showed liquid-crystalline behavior,
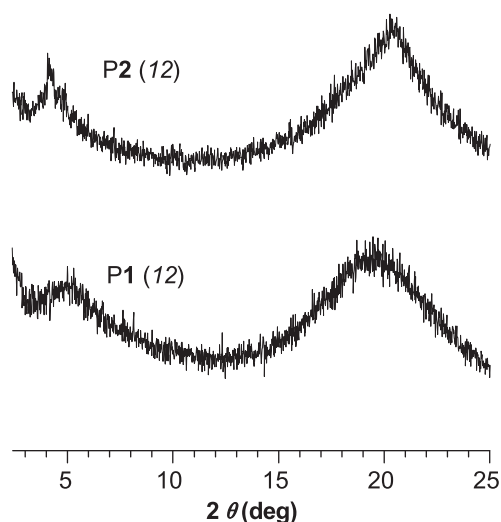

Fig. 12. XRD patterns of liquid-crystalline samples of P2(12) (Table 1, no. 11) and P1(12) (Table 1, no. 7). The samples were heated to 200 °C, cooled to 90 °C for P2(12) and 70 °C for P1(12) at a rate of 5 °C/min, and then kept for 30 min before being rapidly quenched by liquid nitrogen.

as revealed by the POM images (Figures S9 and S10). These results indicate that the length of the flexible spacers plays a key role in the formation of observable mesophases.

Differential scanning calorimetry (DSC) measurements were conducted to evaluate the thermal transition temperatures. Fig. 11 shows the DSC thermograms of P1(12) and P2(12) recorded under nitrogen during the first cooling and second heating scans and the DSC curves for the corresponding monomers are displayed in Figures S11 and S12. In the first cooling circle of P1(12), a sharp exothermic peak associated with i-SmA is observed at 80.8 °C. The mesophase is stable in a temperature range over 8.8 °C before the polymer solidifies at 72.0 °C. The associated g-SmA and SmA-i transitions are observed at 74.8 °C and 87.5 °C, respectively. The transition profiles of P2(12) are similar to those of P1(12). In its first cooling circle, P2(12) enters the SmA phase from its isotropic state at 102.9 °C and the corresponding SmA-i transition is detected at 92.2 °C. The thermal properties of four polymers are summarized in Table 2. It is clear that both P1(6) and P2(6) had only one thermal transition, consistent with the POM results. However, P1(12) and P2(12) owned two transitions, indicative of the existence of liquid-crystalline state.

XRD analyses were performed in an attempt to verify the mesophase assignment and to learn more about the molecular packing. The Bragg reflections at 2θ of 3–5° can be ascribed to the layer spacing of molecular orientational order, and the reflections at 2θ around 20° associate with the intermesogenic organization within the layers [18,20,90]. The appearance of a broad or sharp peak serves as a qualitative indication of the degree of order. As can be seen from Fig. 12, the diffraction pattern of P1(12) shows a diffuse peak centered at $2\theta = 19.46°$, corresponding to an average distance of 4.56 Å (d_2). This distance is associated with the lateral packing arrangement of the azobenzene mesogen. In the small-angle region, a Bragg diffraction at $2\theta = 5.29°$ is observed and the calculated layer distance is 16.69 Å (d_1), which is tentatively assigned to the half of the fully extended molecular length of two layers azobenzene mesogens (see Fig. 13).

As to P2(12), the Bragg diffraction at wide angle region appears at $2\theta = 20.28°$, corresponding to an average distance of 4.38 Å (d_2). It indicates that the lateral packing arrangement of the CF$_3$-azobenzene mesogens is closer than that of azobenzene mesogens (4.56 Å). The observed shorter intermesogen distance can be explained by the fact that the electron-withdrawing effect of the
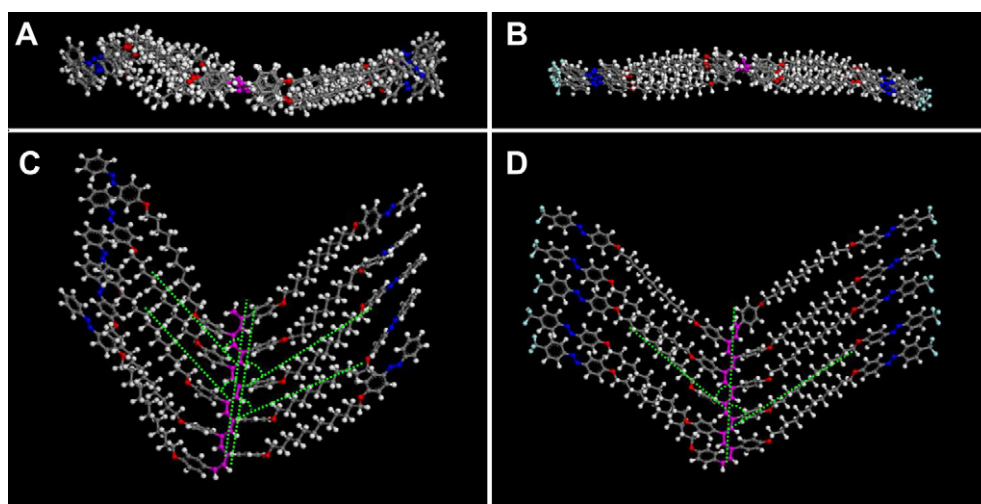
Fig. 13. Illustrations of the molecular configuration after energy minimization: (A) and (B) are top and side view of P1(12), and (C) and (D) are top and side view of P2(12), respectively. Ten repeat units are used in calculation. The carbon, hydrogen, oxygen, nitrogen and fluoride atoms are shown in gray, white, red, blue and green, while the carbon atoms in backbone are shown in pink color. (For interpretation of the references to color in this figure legend, the reader is referred to the web version of this article.)

trifluoromethane group at the end of azobenzene mesogen enhances the molecular dipole and induces the adjacent azo-benzene mesogens to come close. In small-angle region, the diffraction peak centers at $2\theta = 4.06°$, corresponding to an inter-layer distance of 21.75 Å (d_1). This distance is longer than that observed for P1(12), which can be reasonable interpreted by the fact that an CF$_3$-azobenzene mesogen has a larger size than an azobenzene mesogen.

To confirm the analysis of the XRD data and get further insight into the mesogen arrangement in solid states, theoretical calcula-tion has been performed on both to P1(12) and P2(12) with Mate-rials Studio 5.0 program. The calculation results are displayed in Fig. 13. For both P1(12) and P2(12), the side view of the macro-molecular configuration simulated by using 10 repeat units suggests that the side chains stretch out at the two sides of the polyene backbone and they lay in the same plane as the polymer main-chain (Fig. 13A and B). The top views disclose more structural information about molecular packing. As shown by Fig. 13C and D, the side and main-chains of the polymers take a fishbone-like arrangement. For P1(12), the tilt angles between the side chains and main-chain can be largely divided into two groups; the smaller group is averaged to be 41.88°, and the larger one is 54.08° (Fig. 11C). While for P2(12), the average tilted angle is 59.45° (Fig. 13D). In addition, the calculated results also show that the CF$_3$-azobenzenes have higher degree of regularity in mesogen packing than the azobenzenes. These data imply that, in comparison with P1(12), P2(12) has more extended side chains' configuration, and this is in good agreement with the XRD data. Based on the calcu-lation results and experimental data, the smectic structure observed for P1(12) and P2(12) can be illustrated as Fig. 14. A single polymer chain takes a fishbone configuration with a mesogen at the end of each side chain. The mesogens on the adjacent polymer side chains take an interdigital arrangement; such an arrangement results from the dipole–dipole interaction between the adjacent mesogens, which leads to the minimum of total free energy of the whole system. The macromolecular packing shown in Fig. 14 is not
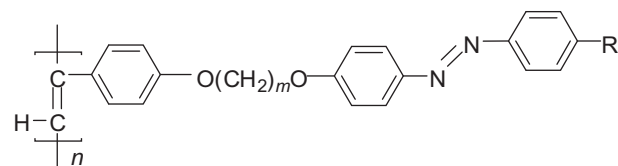
Chart 1.

P1(m) (R=H)
P2(m) (R=CF$_3$)   (m=6, 12)

only in good consistent with the XRD data and simulation results, but also constructive to the formation of smectic liquid crystal mesophase.

4. Conclusions

In summary, a series of azobenzene-containing poly(-phenylacetylene) derivatives (P1(6), P1(12), P2(6), P2(12)) have been successfully synthesized in high yields by using [Rh(nbd)Cl]$_2$ and/or [Rh(cod)Cl]$_2$ as catalysts; their structures have been char-acterized with spectroscopic characterization techniques including FT-IR, ^{1}H NMR, ^{13}C NMR, and UV–visible absorption spectroscopy. Typical photoisomerization behavior was observed for all these azobenzene-containing PPAs by monitoring the feature variations of the UV–visible absorption spectra of the polymer solutions. The rigid PPA main-chain had not prohibited the photoisomerization due to the existence of flexible alkyl spacers between PPA main-chain and the azobenzene moieties, but only lowered the transi-tion rate. The longer alkyl spacer corresponded to a higher isom-erization rate.

The incorporation of azobenzene moieties into polymer side chains also bestowed P1(12) and P2(12) with liquid-crystalline property. The flexibility of the alkyl spacer played a key role in the formation of the mesophase. POM observations indicated that only P1(12) and P2(12) exhibited liquid crystal property, but P1(6) and P2(6) did not, although these two polymer also possessed azo-benzene mesogens. The mesomorphic texture in the POM images suggested that the mesophase formed by P1(12) and P2(12) could be assigned to SmA phase. The phase transition behaviors were measured by DSC technique. The g-SmA and SmA-i transitions observed for P1(12) occurred at 74.8 °C and 87.5 °C, respectively. While for P2(12), it entered the SmA phase from isotropic state at 102.9 °C and the corresponding SmA-i transition was detected at 92.2 °C in the cooling process. The XRD patterns of P1(12) and P2(12) both displayed sharp diffraction peaks, confirming the assignment of SmA phase. The XRD peaks at ~5° and ~20° were correlated with the reflections from ordered layer-by-layer stacking of macromolecules and the ordered packing of adjacent mesogens, respectively. Combining with the theoretical calculation results, an illustration of the molecular arrangement was tentatively proposed. The present investigation not only obtained a few novel azobenzene-functionalized polyphenylacetylene derivatives, but also demonstrated the interdependent properties between three key structural parameters of rigid polymer main-chain, flexible alkyl spacer, and photoisomerization-capable mesogen, thus provides helpful information to the designation and preparation of conjugated polymers with desirable opto-electronic properties.
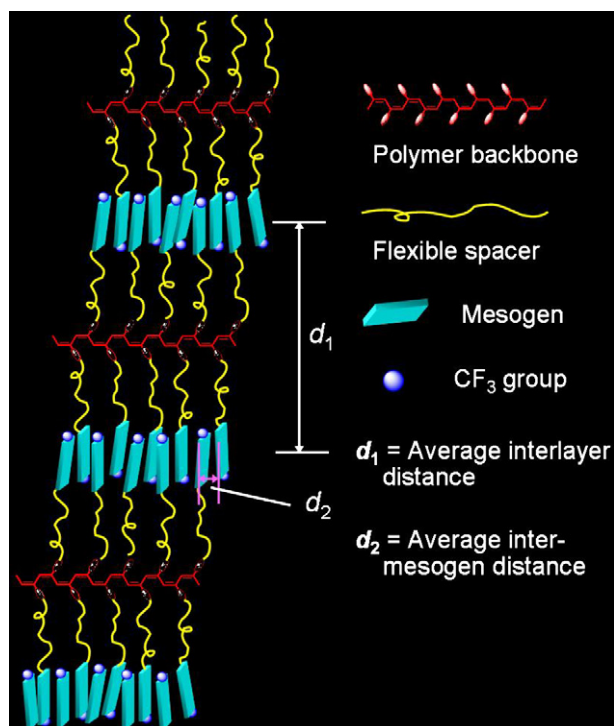
Fig. 14. Schematic presentation of the Smectic A structure of P2(12).

Polymer backbone
Flexible spacer
Mesogen
CF$_3$ group
d_1 = Average interlayer distance
d_2 = Average inter-mesogen distance

Appendix. Supplementary material

Supplementary data associated with this article can be found, in the online version, at doi:10.1016/j.polymer.2011.09.026.

References

[1] Shirakawa H. Angew Chem Int Ed 2001;40:2575–80.
[2] MacDiarmid AG. Angew Chem Int Ed 2001;40:2581–90.
[3] Heeger AJ. Angew Chem Int Ed 2001;40:2591–611.
[4] Lam JWY, Tang BZ. J Polym Sci Part A: Polym Chem 2003;41:2607–29.
[5] Lam JWY, Tang BZ. Acc Chem Res 2005;38:745–54.
[6] Liu JZ, Lam JWY, Tang BZ. Chem Rev 2009;109:5799–867.
[7] Masuda T, Higashimura T. Acc Chem Res 1984;17:51–6.
[8] Nagai K, Masuda T, Nakagawa T, Freeman BD, Pinnau Z. Prog Polym Sci 2001; 26:721–98.
[9] Masuda T. J Polym Sci Part A: Polym Chem 2007;45:165–80.
[10] Akagi K. Chem Rev 2009;109:5354–401.
[11] Yashima E, Maeda K, Iida H, Furusho Y, Nagai K. Chem Rev 2009;109: 6102–211.
[12] Rosen BM, Wilson CJ, Wilson DA, Peterca M, Imam MR, Percec V. Chem Rev 2009;109:6275–540.
[13] Tang BZ, Kong X, Wan X, Feng XD, Kwok HS. Macromolecules 1998;31: 2419–32.
[14] Kong X, Lam JWY, Tang BZ. Macromolecules 1999;32:1722–30.
[15] Lam JWY, Dong Y, Cheuk KL, Luo J, Kwok HS, Tang BZ. Macromolecules 2002; 35:1229–40.
[16] Lam WY, Dong Y, Tang BZ. Macromolecules 2002;35:8288–99.
[17] Lam JWY, Qin A, Dong Y, Lai LM, Haussler M, Dong Y, et al. J Phys Chem B 2006;110:21613–22.
[18] Yuan WZ, Lam JWY, Shen XY, Sun JZ, Mahtab F, Zheng Q, et al. Macromolecules 2009;42:2523–31.
[19] Iftime G, Labarthet FL, Natansohn A, Rochon P. J Am Chem Soc 2000;122: 12646–50.
[20] Zebger I, Rutloh M, Hoffmann U, Stumpe J, Siesler HW, Hvilsted S. J Phys Chem A 2002;106:3454–62.
[21] Tian YQ, Watanabe K, Kong XX, Abe J, Iyoda T. Macromolecules 2002;35: 3739–47.
[22] Zebger I, Rutloh M, Hoffmann U, Stumpe J, Siesler HW, Hvilsted S. Macromolecules 2003;36:9373–82.
[23] Freiberg S, Labarthet FL, Rochon P, Natansohn A. Macromolecules 2003;36: 2680–8.
[24] Gui TL, Jin SH, Park JW, Ahn WS, Koh KN, Kim SH, et al. Opt Mater 2002;21:637–41.
[25] Tong X, Cui L, Zhao Y. Macromolecules 2004;37:3101–12.
[26] Yu YL, Nakano M, Shishido A, Shiono T, Ikeda T. Chem Mater 2004;16: 1637–43.
[27] Rosenhauer R, Fischer T, Stumpe J, Gimenez R, Pinol M, Serrano JL, et al. Macromolecules 2005;38:2213–22.
[28] Sapich B, Vix ABE, Rabe JP, Stumpe P. Macromolecules 2005;38:10480–6.
[29] Deng W, Albouy P, Lacaze E, Keller P, Wang XG, Li MH. Macromolecules 2008; 41:2459–66.
[30] Ding LM, Mao HM, Xu J, He JB, Ding X, Russell TP, et al. Macromolecules 2008; 41:1897–900.
[31] Uekusa T, Nagano S, Seki T. Macromolecules 2009;42:312–8.
[32] Li XJ, Wen RB, Zhang Y, Zhu LR, Zhang BL, Zhang HQ. J Mater Chem 2009;19: 236–45.
[33] Li CS, Lo CW, Zhu DF, Li CH, Liu Y, Jiang HR. Macromol Rapid Commun 2009; 30:1928–35.
[34] Han DH, Tong X, Zhao Y, Galstian T, Zhao Y. Macromolecules 2010;43: 3664–71.
[35] Yoshino T, Kondo M, Mamiya JI, Kinoshita M, Yu YL, Ikeda T. Adv Mater 2010; 22:1361–3.
[36] Yamamoto T, Hasegawa M, Kanazawa A, Shiono T, Ikeda T. J Mater Chem 2000;10:337–42.
[37] Ubukata T, Seki T, Ichimura K. Adv Mater 2000;12:1675–8.
[38] Zettsu N, Ubukata T, Seki T, Ichimura K. Adv Mater 2001;13:1693–7.
[39] Yoneyama S, Yamamoto T, Hasegawa M, Tsutsumi O, Kanazawa A, Shiono T, et al. J Mater Chem 2001;11:3008–13.
[40] Ubukata T, Hara M, Ichimura K, Seki T. Adv Mater 2004;16:220–3.
[41] Zettsu N, Seki T. Macromolecules 2004;37:8692–8.
[42] Bo Q, Yavrian A, Galstian T, Zhao Y. Macromolecules 2005;38:3079–86.
[43] Zettsu N, Ogasawara T, Arakawa R, Nagano S, Ubukata T, Seki T. Macromolecules 2007;40:4607–13.
[44] Isavama J, Nagano S, Seki T. Macromolecules 2010;43:4105–12.
[45] Sobolewska A, Bartkiewicz S, Miniewicz A, Schab-Balcerzak E. J Phys Chem B 2010;114:9751–60.
[46] Li Z, Qin AJ, Lam JWY, Dong YP, Dong YQ, Ye C, et al. Macromolecules 2006;39: 1436–42.
[47] Li ZA, Wu WB, Ye C, Qin JG, Li Z. Polym Chem 2010;1:78–81.
[48] Li ZA, Wu WB, Ye C, Qin JG, Li Z. Macromol Chem Phys 2010;211:916–23.
[49] El Ouazzani H, Iliopoulos K, Pranaitis M, Krupka O, Smokal V, Kolendo A, et al. J Phys Chem B 2011;115:1944–9.
[50] Ho MS, Barrett C, Paterson J, Esteghamatian M, Natansohn A, Rochon P. Macromolecules 1996;29:4613–8.
[51] Andruzzi L, Hvilsted S, Ramanujam PS. Macromolecules 1999;32:448–54.
[52] Wu YL, Natansohn A, Rochon P. Macromolecules 2004;37:6090–5.
[53] Li YB, He YN, Tong XL, Wang XG. J Am Chem Soc 2005;127:2402–3.
[54] Goldenberg LM, Kulikovska O, Stumpe J. Langmuir 2005;21:4794–6.
[55] Gao J, He YN, Xu HP, Song B, Zhang X, Wang ZQ, et al. Chem Mater 2007;19: 14–7.
[56] Gao J, He YN, Liu F, Zhang X, Wang ZQ, Wang XG. Chem Mater 2007;19: 3877–81.
[57] Sobolewska A, Miniewicz A. J Phys Chem B 2007;111:1536–44.
[58] Nakano H, Tanino T, Takahashi T, Ando H, Shirota Y. J Mater Chem 2008;18: 242–6.
[59] Lee J, Kim M, Nakayama T. Langmuir 2008;24:4260–4.
[60] Priimagi A, Lindfors K, Kaivola M, Rochon P. Appl Mater Interf 2009;1:1183–9.
[61] Xue XQ, Zhu J, Zhang ZB, Zhou NC, Tu YF, Zhu XL. Macromolecules 2010;43: 2704–12.
[62] Goldenberg LM, Kulikovsky L, Kulikovsky O, Tomczyk J, Stumpe J. Langmuir 2010;26:2214–7.
[63] Harbron EJ, Vicente DA, Hoyt MT. J Phys Chem B 2004;108:18789–93.
[64] Harbron EJ, Vicente DA, Hadley DH, Imm MR. J Phys Chem A 2005;109: 10846–53.
[65] Grimes AF, Call SE, Vicente DA, English DS, Harbron EJ. J Phys Chem B 2006; 110:19183–90.
[66] Lewis SM, Harbron EJ. J Phys Chem C 2007;111:4425–30.
[67] Harbron EJ, Hadley DH, Imm MR. J Photochem Photobiol A: Chem 2007;186: 151–7.
[68] Grimes AF, Call SE, Harbron EJ, English DS. J Phys Chem C 2007;111: 14257–65.
[69] Tomatsu I, Hashidzume A, Harada A. J Am Chem Soc 2006;128:2226–7.
[70] Pouliquen G, Amiel C, Tribet C. J Phys Chem B 2007;111:5587–95.
[71] Fujii T, Shiotsuki M, Inai Y, Sanda F, Masuda T. Macromolecules 2007;40: 7079–88.
[72] Ruchmann J, Fouilloux S, Tribet C. Soft Matter 2008;4:2098–108.
[73] Zhao YL, Stoddart JF. Langmuir 2009;25:8442–6.
[74] Chen X, Hong L, You X, Wang YL, Zou G, Su W, et al. Chem Commun; 2009:1356–8.
[75] Natansohn A, Rochon P. Chem Rev 2002;102:4139–75.
[76] Schultz T, Quenneville J, Levine B, Toniolo A, Martinez TJ, Lochbrunner S, et al. J Am Chem Soc 2003;125:8098–9.
[77] Ikegami T, Kurita N, Sekino H, Ishikawa Y. J Phys Chem A 2003;107:4555–62.
[78] Loudwig S, Bayley H. J Am Chem Soc 2006;128:12404–5.
[79] Francesca S, Eugene MT. Macromolecules 2008;41:981–6.
[80] Uchida K, Yamaguchi S, Yamada H, Akazawa M, Katayama T, Ishibashi Y, et al. Chem Commun; 2009:4420–2.
[81] Yu B, Jiang X, Wang R, Yin J. Macromolecules 2010;43:10457–65.
[82] Lee KM, Koerner H, Vaia RA, Bunning TJ, White TJ. Macromolecules 2010;43: 8185–90.
[83] Chen W, Wei X, Balazs AC, Matyjaszewski K, Russell TP. Macromolecules 2011;44:1125–31.
[84] Tang BZ, Poon WH, Leung SM, Leung WH, Peng H. Macromolecules 1997;30: 2209–12.
[85] Masuda T, Tang BZ, Higashimura T, Yamaoka H. Macromolecules 1985;18: 2369–73.
[86] Yuan WZ, Sun JZ, Dong YQ, Häußler M, Yang F, Xu HP, et al. Macromolecules 2006;39:8011–20.
[87] Yuan WZ, Mao Y, Zhao H, Sun JZ, Xu HP, Jin JK, et al. Macromolecules 2008;41: 701–7.
[88] Yuan WZ, Sun JZ, Liu JZ, Dong Y, Li Z, Xu HP, et al. J Phys Chem B 2008;112: 8896–905.
[89] Zhao H, Yuan WZ, Tang L, Sun JZ, Xu H, Qin A, et al. Macromolecules 2008;41: 8566–74.
[90] Liu LM, Liu KP, Dong YP, Chen EQ, Tang BZ. Macromolecules 2010;43: 6014–23.